Materials Today: Proceedings xxx (xxxx) xxx

Contents lists available at ScienceDirect

Materials Today: Proceedings

journal homepage: www.elsevier.com/locate/matpr

Preparation and characterization of zinc–borate glasses doped with Ag_2O

K.M. Shwetha, B Eraiah *

Department of Physics, Banglore University, Bangalore-560056, Karnataka, India

ARTICLE INFO

Article history:
Available online xxxx

Keywords:
Energy band gap
Density
Silver chloride
Borate glass

ABSTRACT

Using the melt quenching approach, glasses having the formula $ZnO\text{-}B_2O_3\text{-}Ag_2O$ have been created. Utilising the X-ray diffraction technique, the synthesized glass has been described. The Archimedes method was used to compute the densities of these glasses,and the appropriate formula was used to determine the associated molar volume.Absorption spectra were recorded using a UV–visible spectrometer.Tauc's figure has been used to examine the energy band gap.Ag_2O concentration-related variations in band gap energy have been discussed.

Selection and peer-review under responsibility of the scientific committee of the 2nd International Conference on Multifunctional Materials.

1. Introduction

Borate glasses are excellent glass makers because they have a crucial quality called optical transparency from the near infrared and visible range. Photonic and opto-electronic devices use B_2O_3 glasses[1,2].Due to its internal structure's non-bridging oxygen atoms, the borate glasses combined with alkali oxides like ZnO will be re-arranged.[3]ZnO has two functions: one at high coyncentrations it forms glass, and another at low concentrations it modifies glass.Since ZnO is neither hygroscopic nor toxic, it aids in reducing the moisture content of borate glasses[4]. Glass modifier features linked to ionic bonding and network forming behaviour linked to covalent bonding[2,5]. When doped with ZnO, Nobel metals like Ag, Au, and Cu will become neutral atoms at high temperatures. (See Table 1).

2. Experimental

2.1. Synthesis of sample

Samples that have general formula $60B_2O_3\text{-}(40\text{-}x)ZnO\text{-}xAg_2O$ (ZBA) (where x = 0,1.0,1.5,2,2.5. mol %) fabricated by by melt quenching method. The raw materials were used in the glass synthesis are B_2O_3,ZnO,Ag_2O were weighed in a electrical microbalance and powdered,mixed thoroughly using mortar and pestle.The mixture containing cruicible was placed in a furnace and after one hour at1150°C homogeneous mixture was quenched at room temperature in between two brass moulds.The obtained samples are annealed at around 300^0c for 1 h to eliminate thermal stress and strain developed during quenching.

2.2. Density and molar volume

Densities of prepared glasses were measured by Archimedes principle, using toluene as standard immersion liquid. The corresponding molar volume was calculated using appropriate formula.

2.3. Optical properties

The absorption spectra was obtained in a UV visible spectrometer of model UV-1800 Shimadzu spectrometer,in the range of wavelength 200 nm to 1100 nm at room temperature.

2.4. X- ray diffraction study

The X-rd spectra of these samples was recorded using an instrument Rigaku X-ray diffractometer in between 10^0 to 80^0 in 2θ range.

2.5. FTIR study

To know the functional group of the glass samples the FTIR (Fourier infrared spectrometer) spectra was recorded using instrument, Parkinson Elmer from the range 500 cm^{-1} to 4000 cm^{-1}

* Corresponding author.
E-mail addresses: eraiah@rediffmail.com, beraiah@bub.ernet.in (B Eraiah).

https://doi.org/10.1016/j.matpr.2023.05.159
2214-7853/
Selection and peer-review under responsibility of the scientific committee of the 2nd International Conference on Multifunctional Materials.

Table 1
Functional groups for ZBA glasses.

3600–3750	OH– group[23-25]
3200–3500	Molecular water
700–3000	Hydrogen bonding [21,24]
1346–1377	B–O asymmetric stretching of trigonal bond [22]
1234	BO3 unit B–O stretching vibrations of bond$(BO3)^{3-}$[23]
993	Stretching vibration of B–O–Zn linkage[10]
670	Zn–O bond vibrations and O–B-O Bond bending Vibrations.[21]

3. Results and evaluation

3.1. Analysis of X-ray diffraction

The spectra of glasses made of zinc-borate and Ag_2O are displayed in Fig. 1. There are no peaks to be seen in the picture, and the presence of a hump at 32.74^0 and 57.37^0 confirms that the material is glass.

3.2. Molar volume and density

Fig. 2 displays the variation in molar volume and density with mol% Ag_2O.When there are non-bridging oxygens present, density increases after decreasing by up to 2 mol% for Ag_2O. As expected, the molar volume rises with an increase in Ag_2O mol% up to 1.5 mol% before falling.These glasses' densities were assessed using a relation.

$$\rho = \frac{ma}{(ma - ml)} X\rho_T \quad (1)$$

Where ρ_T = toulene density and ma and ml are the sample's masses in the liquid and the air, respectively.

$$The formula V = M/\rho_T \quad (2)$$

was used to compute the molar volume, where M stands for the samples' molecular weights. where ρ_T is toluene's density (at room temperature), which is 0.866 g/cm^3.

3.3. Analysis of optical absorption spectra

ZBA glasses' absorption spectra, as shown in Fig. 3.

$$\alpha(\upsilon) = 2.303 * Ab/t \quad (3)$$

was used to determine the optical absorption co-efficient

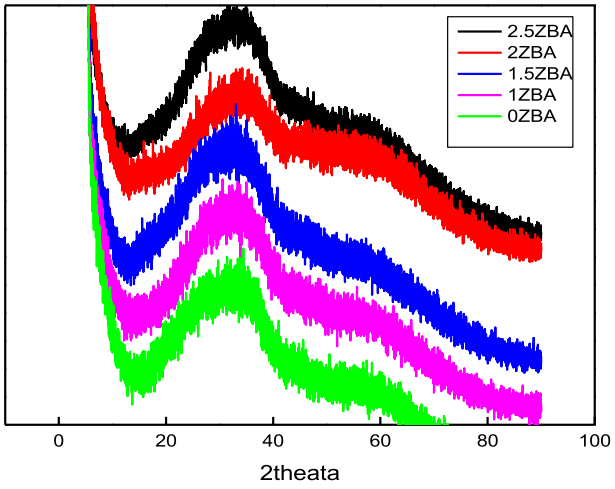

Fig. 1. X-ray Diffraction spectra of ZBA glasses.

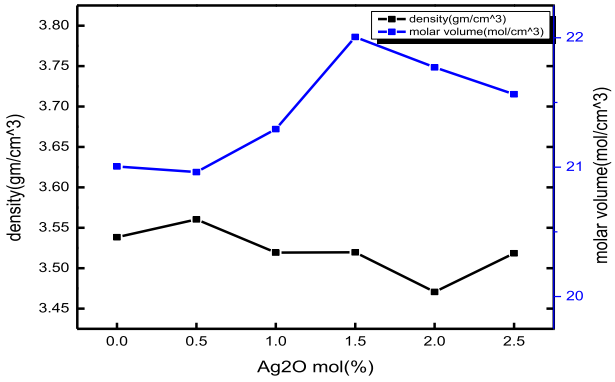

Fig. 2. The change of density with mol%of Ag_2O.

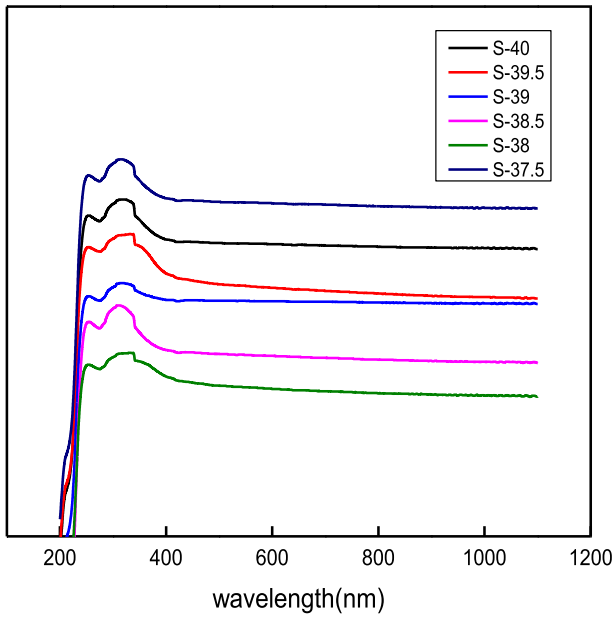

Fig. 3. Optical obsorption spectra.

where the sample's thickness is t and the absorptance is Ab. Tauc's figure has been used to compute the band gap energy[6,7]. Base glass exhibits an absorption peak at 365 nm; this peak may be caused by Zn^{2+} ions[8]. With the addition of Ag_2O concentration, the degree of intensity of the absorption spectra increases.The wavelengths of the Ag^{2+} ion's observed peaks are 220, 340, and 370 nm.

3.4. Eopt, the optical energy band gap

The absorption co-efficient has been calculated using UV–visible spectra and tauc's plot[6,9]. Utilising the relationship, the direct and indirect band gaps have been calculated.

$\alpha h\nu = B(h\nu - E_{opt})$

$$E_{opt} = h\vartheta - \left(\frac{\alpha h\nu}{B}\right)^{1/2} \quad (4)$$

where 'B' is a fixed value, n = 1/2 and 2 for band gaps, both direct and indirect respectively, Eopt is the optical energy, while hυ is the incident photon energy.

energy band gap.Calculated and visualised using (hυ) v/s αhυ was the indirect and direct band gap energy. Figs. 4 and 5 show an indirect and direct version of the Tauc's plot, a typical graph

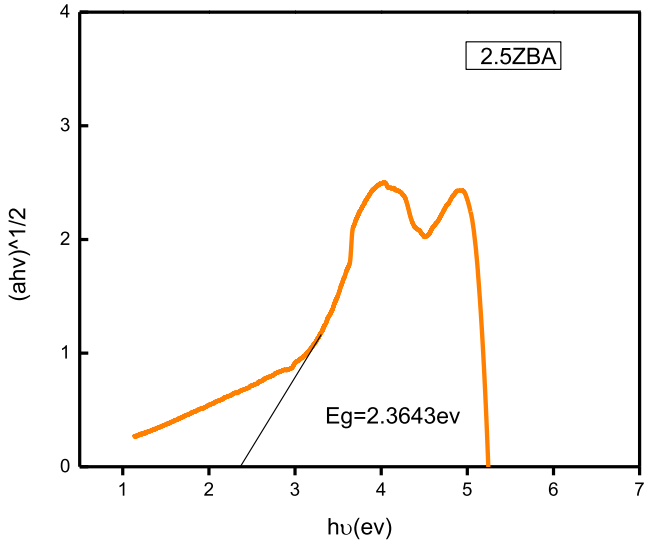

Fig. 4. $(\alpha h\nu)^{1/2}$ v/s hν optical indirect energy band gap.

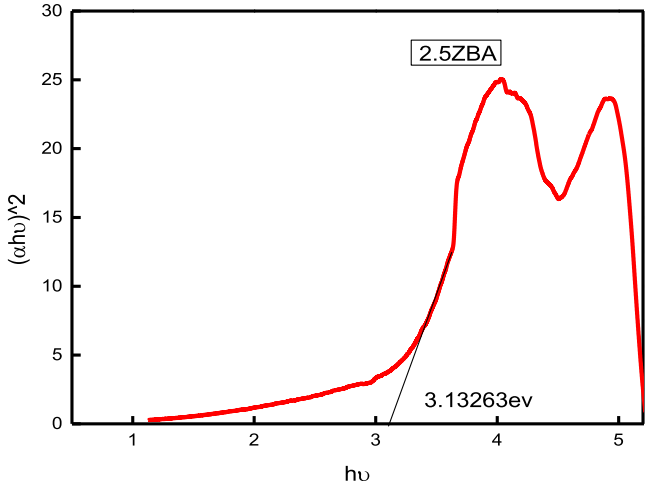

Fig. 5. $(\alpha h\nu)^2$ vs hν optical direct energy band gap.

for the energy band gap. According to Fig. 6, the addition of more non-bridging oxygen atoms from 0 mol% to 2.5 mol% causes the energy band gap to widen as Ag_2O mol%.Due to a change in the structure of the glass network, there is a modest decrease in the energy band gap at 2 mol%.When a little amount of Ag_2O is introduced into a host glass network, the energy band gap widens by up to 1.5 mol% as a result of the breakage of Zn-B-O bonds, which results in a decrease in Eopt values of 2 mol%.[10].

3.5. Urbach energy

The definition of urbach energy (u) is to understand the degree of disorder in amorphous material. The following relationship is given:

$$Ln\alpha = lno + expU \quad (5)$$

where α is a absorption coefficient. Plotting ln(α) v/s (hν) photon energy and taking into account the inverse slope of the linear component of the curves, (U) has been determined.The computed urbach energy is presented in Table 2 with the notation u and the values of the optical energy band are diametrically opposed.The growth of the width of the delocalized states has been used to explain the rising order of urbach energy.The process of electron–phonon relaxation within the glass structure may be the cause of the optical absorption edge's expansion [11].

3.6. FTIR research

Fig. 7. Fourier transform infrared spectra with wave numbers between 500 and 4000 cm^{-1} were detected at room temperature. From the fig, it can be seen that the metal cat ion vibrations of Ag^{2+} or ZnO bonds are responsible for the 500 cm^{-1} absorption band[12,13,27].Ag_2O vibrational bonds are the cause of the band at 605 cm^{-1}.The vibrational bending of B-O-B connections in BO_4 triangles is what causes the band at 697 cm^{-1} [14,18].The lengthening of vibrations in B-O from BO_4 units is what causes the absorption band at 877 cm^{-1} and 939 cm^{-1}.The B-O vibrational stretching in of BO_4 units from various tri, tetra, and penta borate groups is what causes the peak at 1054 cm^{-1} is caused by the BO_4 units from different tetra, penta, and tri borate groups entering the B-O vibrational stretching [15-17].The vibrational stretching of B-O in BO_3 units is the cause of the peak at 1278 cm^{-1}.The band with centres at 1000 cm^{-1} and 1100 cm^{-1} due to the vibrations of the triborate, pentaborate, and $(BO_4)^{4-}$ tetrahedral group [19].The asymmetric and symmetric stretching of the H_2O molecule is what causes the bands to be present at 2098 cm^{-1} and 3325 cm^{-1}[20]. The peak at 2975 $cm^{-1,}$ which was caused by O–H group vibrational stretching, proves that glass samples are hygroscopic by virtue of the presence of O–H groups in their network[10,21,22,28].

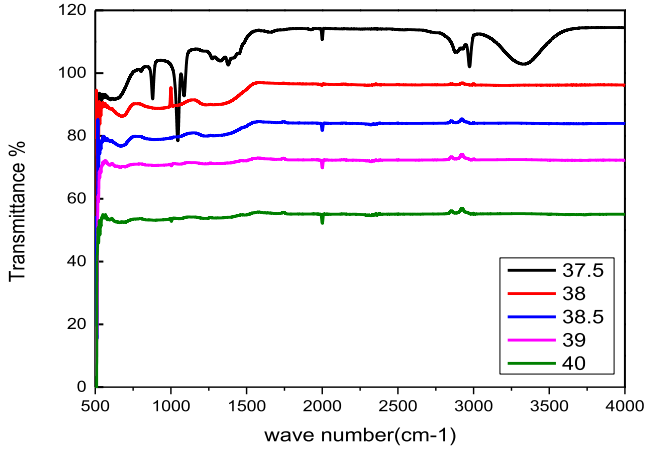

Fig. 6. Shows the FTIR spectra of prepared glass sample.

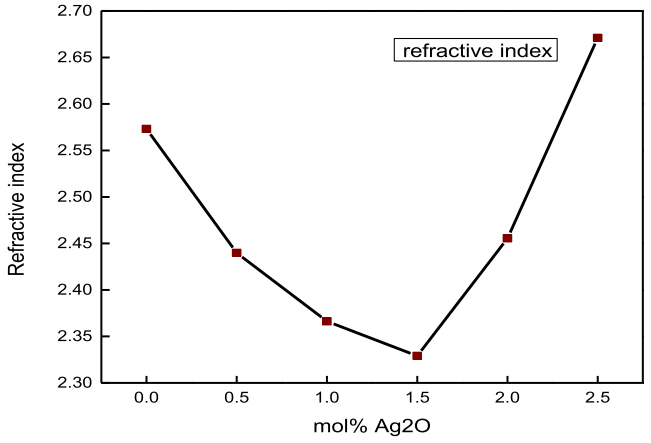

Fig. 7. Refractive index vs mol% Ag_2O.

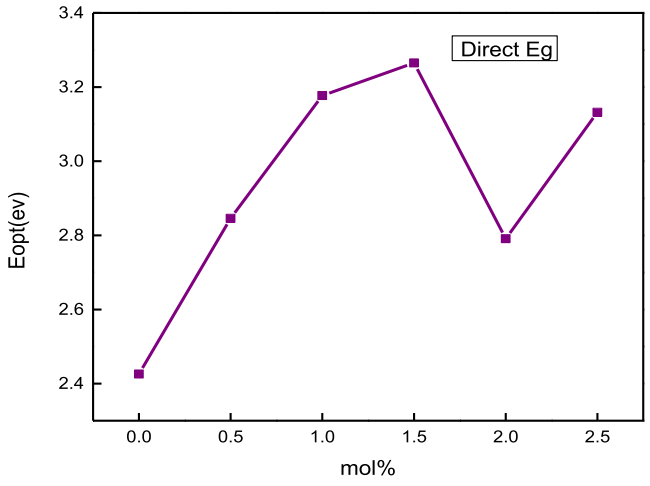

Fig. 8. Optical energy gap with respect to concentration Ag2O of ZBA sample.

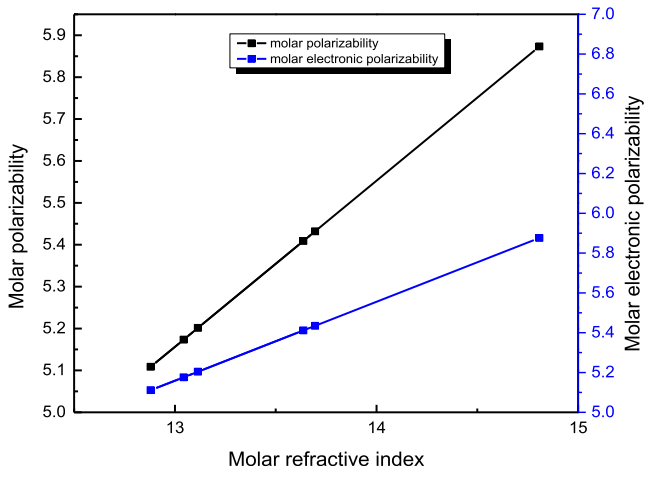

Fig. 9. Molar polarization v/s molar electronic polarization.

3.7. Index of refraction (n)

The following Dimitrov and Sakka equation [23] the ability to determine the refractive index from energy band gap measurements.

$$\sqrt{\mathrm{Eg}/20} = \frac{n^2-1}{n^2+2} \rightarrow \mathrm{n} = \left(\frac{3-2(\sqrt{Eg/20})}{\sqrt{Eg/20}}\right)^{1/2} \quad (6)$$

n is the refractive index. Energy band gap, Eg

Fig. 7 illustrates how the computed refractive index changes as Ag_2O concentration does. because there are more non-bridging oxygen atoms, the refractive index increases with concentration of Ag_2O at 1.5 mol% after initially decreasing up to 1.5 mol% due to the existence of less oxygen atoms that do not bridge.Fig. 8.

3.8. Molar polarizability (m), molar electronic polarizability (me), and molar refraction (Rm)

Using the Lorentz-Lorentz equation presented below[24,25], the molar refraction, molar electronic polarizability, and molar polarizability for these glasses were calculated.

$$me = R_m(2.52) \quad (7)$$

$$\mathrm{R_m} = \frac{n^2-1}{n^2+2} \quad (8)$$

$$\mathrm{m} = \left[\frac{3}{4\pi \mathrm{NA}}\right] \times \mathrm{Rm} \quad (9)$$

Where n, Vm, and Rm stand for the refractive index, molar volume, and molar refractivity, respectively, and N is the Avogadro number (6.022x1023).According to Fig. 9, both m and me are dependent on Rm and have a strong relationship to one another when the concentration of Ag2O is substituted.With an increase in Ag_2O concentration, the number of non-bridging oxygen atoms results in a decrease in molar polarizability, molar electronic polarizability, and molar refraction.[26] Table 2 lists all the calculated values.

4. Conclusion

Glasses made of $ZnO\text{-}B_2O_3\text{-}Ag_2O$ have been successfully created utilising the melt-quenching technique.XRD was used to determine whether these samples were amorphous. The non-bridging oxygen atoms found in the glass network were used as a basis for discussing the variation in molar volume and density with Ag_2O mol%.Using Tauc's plots, the band gap energy values were calculated.These glasses' energy band gap values show that they can be used in optical electrical and display device applications.

CRediT authorship contribution statement

K.M. Shwetha: . **B Eraiah:** Conceptualization, Formal analysis, Methodology, Project administration, Supervision, Writing – review & editing.

Table 2
Density (ρ), molar volume V(m), direct (Eopt) and indirect (E′ opt) band gap, refractive index (n) and molar polarizability (αm),electronic polarizability(α_e),dielectric constant(ϵ) reflection loss(Rl), optical transmission(Topt±0.002).

Sample	0ZBA	1ZBA	1.5ZBA	2ZBA	2.5ZBA
Concentration of samples(Ag2O)	0	1	1.5	2	2.5
Thickness(cm)	0.399	0.2633	0.27833	0.2696	0.3263
Density(ρ)$gm/cm3$	3.5383	3.5193	3.5196	3.4706	3.7849
Molar volume(Vm)(mol/cm3)	21.005	21.294	22.006	21.771	20.050
Direct band gap Eg(ev) ± 0.001	2.426	3.177	3.265	2.791	3.132
Indirect band gap Eg(ev) ± 0.001	2.497	2.480	2.468	2.354	2.601
Refractive index(n)(direct)	2.573	2.366	2.329	2.455	2.671
Molar refraction(Rm) ± 0.001	13.695	12.880	13.114	13.637	14.808
MolarPolarizability(αm) ± 0.001x10^-24 cm^3	5.433	5.1086	5.2010	5.4085	5.8732
Molar Electronic polarizability(α_{me}) ± 0.001	5.4346	5.111	5.2039	5.4115	5.8761
Dielectric constant (∈)	6.6208	5.5989	5.4247	6.0294	7.1342
Urbach energy(Δu)	6.2038	8.1685	5.6831	4.3996	4.8302

Data availability

Data will be made available on request.

Declaration of Competing Interest

The authors declare that they have no known competing financial interests or personal relationships that could have appeared to influence the work reported in this paper.

References

[1] Y.B. Saddeek, J. Alloys Compd. 467 (2009) 14–21.
[2] R. Ciceo-Lucacel, I. Ardelean, J. Non-Cryst, Solids 353 (2007) 2020–2024.
[3] Y.B. Saddeek, L.A.E. Latif, Physica B 348 (2004) 475–484.
[4] R.J. Amjad, M.R. Sahar, S.K. Ghoshal, M.R. Dousti, S. Riaz, A.R. Samavati, M.N.A. Jamaludin, S. Naseem, Chin. Phys. Lett. 30 (2013) 027301.
[5] G. El-Damrawi, E. Mansour, Physica B 364 (2005) 190–198.
[6] E.A. Davis, N.F. Mott, J. Philos. Mag. 22 (1970) 903–922.
[7] M.S. Al-Buriahi, Y.S.M. Alajerami, A.S. Abouhaswa, TaninNutaro Amani Alalawi, Baris J. Non- Cryst. Solids **544** (2020) 120171.
[8] B.Eraiah, Roopa, J. Non Cryst. Solids **551** (2021) 120394.
[9] B. Eraiah, Bull. Mater. Sci. 29 (2006) 375–378.
[10] M. El-Hagary, E.R. Shaaban, S.H. Moustafa, G.M.A. Gad, Solid State Sci. 91 (2019) 15–22.
[11] S.A. Fayek, M.R. Balboul, K.H. Marzouk, Thin. S Films 515 (2007) 7281–7285.
[12] A.K. Yadav, C.R. Gautam, A. Gautam, V.K. Mishra, Phase Transitions 86 (2013) 1000.
[13] G. Padmaja, P. Kistaiah, J. Phys. Chem. A 113 (2009) 2397.
[14] G.P. Singh, Parvinder Kaur, Simranpreet Kaur, D.P. Singh, Mater. Phys. Mech. **12** (2011) 58.
[15] S.R. Rejisha, N. Santha, J. Non-Cryst. Solids 357 (2011) 3813.
[16] R. Stefan, E. Culea, P. Pascuta, J. Non-Cryst. Solids 358 (2012) 839.
[17] Pavan Kumar Pothuganti, Ashok Bhogi, Muralidhara Reddy Kalimi, Padamasuvarna Reniguntla, Glass Phys. Chem. **46** (2020) 146.
[18] N. Krishnamacharyulu, G. Jagan Mohini, G. Sahaya Baskaran, V. Ravi Kumar, N. Veeraiah, J. Non Cryst. Solids 452 (2016) 23–29.
[19] E. Mansour, J. Mol. Strut. 1014 (2012) 1–6.
[20] Kaushal Jha, M. Jayasimhadri, J. Alloys Compd. **688** (2016) 833–840.
[21] M.K. Halimah, S.A. Umar, K.T. Chan, A.A. Latif, M.N. Azlan, A.I. Abubakar, A.M. Hamza, Mater. Chem. Phys. 238 (2019).
[22] F. Urbach, Phys. Rev. 92 (1953) 1324–1330.
[23] V. Dimitrov, S. Sakka II, J. Appl. Phys. 79 (1996) 1741–1745.
[24] S.B. Kolavekar, N.H. AyachitMater, Chem. Phys. 257 (2021).
[25] R.A. Tafida, M.K. Halimah, F.D. Muhammad, K.T. Chan, M.Y. Onimisi, A. Usman, A.M. Hamza, S.A. Umar,Structural, Mater Chem. Phys. **246** (2020), 122801
[26] A.A. Ali, Y.S. Rammah, M.H. Shaaban, J. Non - Cryst. Solids 514 (2019) 52–59.
[27] Ashok Bhogi, B. Srinivas, Padmavathi Papolu, Md Shareefuddin, P. Kistaiah, Materials Chemistry and Physics,Volume **291**(2022),126698,ISSN 0254-0584.
[28] Ashok Bhogi, Boora Srinivas, Papolu Padmavathi, Kasarapu Venkataramana, Kiran Kumar Ganta, Mohd Shareefuddin, Puram Kistaiah,Volume **133** (2022),112911,ISSN 0925-3467.